



S-Palmitoylation of Tyrosinase at Cysteine⁵⁰⁰ Regulates Melanogenesis

Niki, Yoko ; Adachi, Naoko ; Fukata, Masaki ; Fukata, Yuko ; Oku, Shinichiro ; Makino-Okamura, Chieko ; Takeuchi, Seiji ; Wakamatsu, ...

(Citation)

Journal of Investigative Dermatology, 143(2):317-327

(Issue Date)

2023-02

(Resource Type)

journal article

(Version)

Version of Record

(Rights)

© 2022 The Authors. Published by Elsevier, Inc. on behalf of the Society for Investigative Dermatology.

Creative Commons Attribution 4.0 International license

(URL)

<https://hdl.handle.net/20.500.14094/0100481846>



S-Palmitoylation of Tyrosinase at Cysteine⁵⁰⁰ Regulates Melanogenesis



JID Open

Yoko Niki^{1,2,8}, Naoko Adachi^{3,8}, Masaki Fukata⁴, Yuko Fukata⁴, Shinichiro Oku⁴, Chieko Makino-Okamura¹, Seiji Takeuchi^{1,5}, Kazumasa Wakamatsu⁶, Shosuke Ito⁶, Lieve Declercq⁷, Daniel B. Yarosh⁷, Tomas Mammone⁷, Chikako Nishigori⁵, Naoaki Saito^{1,3} and Takehiko Ueyama³

Palmitoylation is a lipid modification involving the attachment of palmitic acid to a cysteine residue, thereby affecting protein function. We investigated the effect of palmitoylation of tyrosinase, the rate-limiting enzyme in melanin synthesis, using a human three-dimensional skin model system and melanocyte culture. The palmitoylation inhibitor, 2-bromopalmitate, increased melanin content and tyrosinase protein levels in melanogenic cells by suppressing tyrosinase degradation. The palmitoylation site was Cysteine⁵⁰⁰ in the C-terminal cytoplasmic tail of tyrosinase. The nonpalmitoylatable mutant, tyrosinase (C500A), was slowly degraded and less ubiquitinated than wild-type tyrosinase. Screening for the Asp-His-His-Cys (DHHC) family of proteins for tyrosinase palmitoylation suggested that DHHC2, 3, 7, and 15 are involved in tyrosinase palmitoylation. Knockdown of DHHC2, 3, or 15 increased tyrosinase protein levels and melanin content. Determination of their subcellular localization in primary melanocytes revealed that DHHC2, 3, and 15 were localized in the endoplasmic reticulum, Golgi apparatus, and/or melanosomes, whereas only DHHC2 was localized in the melanosomes. Immunoprecipitation showed that DHHC2 and DHHC3 predominantly bind to mature and immature tyrosinase, respectively. Taken together, tyrosinase palmitoylation at Cysteine⁵⁰⁰ by DHHC2, 3, and/or 15, especially DHHC2 in *trans*-Golgi apparatus and melanosomes and DHHC3 in the endoplasmic reticulum and *cis*-Golgi apparatus, regulate melanogenesis by modulating tyrosinase protein levels.

Journal of Investigative Dermatology (2023) 143, 317–327; doi:10.1016/j.jid.2022.08.040

INTRODUCTION

Melanocytes synthesize melanin, a pigment responsible for human skin, hair, and eye color, which provides protection against UV irradiation. Melanin is synthesized in a specialized lysosome-related organelle, the melanosome (Serre et al., 2018), which transfers melanin polymers from melanocytes to the surrounding keratinocytes (KCs) in the human skin (Ando et al., 2012). Mammalian melanocytes synthesize two types of melanin: black eumelanin and yellow–red pheomelanin (Ito and Wakamatsu, 2008). Melanin synthesis in mammalian melanocytes is controlled by three

melanogenic enzymes: tyrosinase, TYRP-1, and TYRP-2 (Lai et al., 2018). Tyrosinase is the rate-limiting enzyme that catalyzes the first step in the melanin synthesis pathway, from tyrosine to DOPAquinone, which is spontaneously converted to DOPACHROME (Supplementary Figure S1a). In mouse melanocytes, Tyrp-2 and Tyrp-1 regulate the late stages of eumelanin synthesis by regulating the tautomerization of DOPACHROME to 5,6-dihydroxyindole-2-carboxylic acid (Tsukamoto et al., 1992) and the oxidation of 5,6-dihydroxyindole-2-carboxylic acid to *o*-quinone (Kobayashi et al., 1994), respectively. In human melanocytes, 5,6-dihydroxyindole-2-carboxylic acid is oxidized by tyrosinase. The 5,6-dihydroxyindole-2-carboxylic acid, 5,6-dihydroxyindole (a spontaneously oxidized DOPACHROME), and the corresponding *o*-quinones undergo relatively intermixed polymerization to form eumelanin (Ito and Wakamatsu, 2008).

Tyrosinase, a copper-containing type I membrane glycoprotein, is initially synthesized in the endoplasmic reticulum (ER) and matured through complex sugar modifications in the Golgi apparatus. Thereafter, tyrosinase traffics to melanosomes through the *trans*-Golgi network through the endosome pathways (Ohbayashi and Fukuda, 2020). Intracellular tyrosinase levels affect melanin synthesis and pigmentation and are controlled by a balance between tyrosinase synthesis and degradation. Several intrinsic factors, such as TGF- β 1 (Martínez-Esparza et al., 1997), TNF- α (Martínez-Esparza et al., 1998), linoleic acid (Ando et al., 2006), phospholipase D2 (Kageyama et al., 2004), terrain (Park et al., 2009), and 1-(2,4-dihydroxyphenyl)-3-(2,4-dimethoxy-3-methylphenyl) propane (Niki et al., 2011), regulate melanin synthesis by

¹Kobe Skin Research Department, Biosignal Research Center, Kobe University, Kobe, Japan; ²School of Pharmacy and Pharmaceutical Sciences, Mukogawa Women's University, Nishinomiya, Japan;

³Laboratory of Molecular Pharmacology, Biosignal Research Center, Kobe University, Kobe, Japan; ⁴Division of Membrane Physiology, Department of Molecular and Cellular Physiology, National Institute for Physiological Sciences, National Institutes of Natural Sciences, Aichi, Japan; ⁵Division of Dermatology, Department of Internal Related, Graduate School of Medicine, Kobe University, Kobe, Japan; ⁶Institute for Melanin Chemistry, Fujita Health University, Aichi, Japan; and ⁷Research & Development, Estee Lauder Companies, Melville, New York, USA

⁸These authors contributed equally to this work.

Correspondence: Takehiko Ueyama, Laboratory of Molecular Pharmacology, Biosignal Research Center, Kobe University, Rokkodai-cho 1-1, Nada-ku Kobe 657-8501, Japan. E-mail: tueyama@kobe-u.ac.jp

Abbreviations: 2-BP, 2-bromopalmitate; Cys or C, Cysteine; DHHC, Asp-His-His-Cys; endo H, endoglycosidase H; ER, endoplasmic reticulum; HA, hydroxylamine; KC, keratinocyte; NHEM, normal human epidermal melanocyte; siRNA, small interfering RNA; WT, wild-type

Received 27 February 2022; revised 9 August 2022; accepted 10 August 2022; accepted manuscript published online 5 September 2022; corrected proof published online 12 October 2022

modulating tyrosinase degradation. Tyrosinase is degraded through the ubiquitin–proteasome system (Ando et al., 2009; Bellei et al., 2010) and/or the endosomal/lysosomal system (Fujita et al., 2009). Carbohydrate modification studies have revealed that tyrosinase is degraded by proteasomes through ER-associated protein degradation (Svedine et al., 2004).

S-Palmitoylation (palmitoylation), a reversible lipid modification, involves the attachment of long-chain fatty acid groups (predominantly palmitate, C16:0) to specific cysteine (Cys or C) residues through thioester linkages and occurs in the cytoplasmic face of membranes (Resh, 2006). Palmitoylation modifies several hundreds of soluble and integral membrane proteins, including enzymes (Martin and Cravatt, 2009; Yang et al., 2010). Palmitoylation affects substrate protein hydrophobicity and regulates membrane binding, protein–protein interactions, protein stability, localization, and trafficking (Chamberlain and Shipston, 2015; Fukata and Fukata, 2010; Linder and Deschenes, 2007). Palmitoylation is catalyzed by a family of palmitoyl acyl transferase enzymes containing an Asp-His-His-Cys (DHHC)-rich domain that is directly involved in the palmitoyl transfer reaction (Mitchell et al., 2006). The DHHC domain is highly conserved in organisms from *Saccharomyces cerevisiae* to mammals, and mutations in this domain abolish its palmitoyl transferase activity (Yang et al., 2010). A family of 23 mammalian DHHC proteins was characterized, and progress has been made in identifying their substrates and characterizing their expression patterns (<http://biogps.org/> and <https://gtexportal.org/home/>) and subcellular localization (Fukata et al., 2004; Ohno et al., 2006). However, palmitoylation of tyrosinase has not yet been reported.

In this study, we investigated the effect of tyrosinase palmitoylation on melanogenesis.

RESULTS

Palmitoylation inhibitor increases melanin content in a human skin model and melanocytes

To investigate the role of palmitoylation in human skin, a palmitoylation inhibitor, 2-bromopalmitate (2-BP), was incubated with a human three-dimensional skin model system. Macroscopic views of the skin model after 2-BP treatment for 17 days showed increased pigmentation compared with that of the control (DMSO) (Figure 1a). The total amount of eumelanin and pheomelanin in the 2-BP-treated skin model was significantly higher than that in the control (Figure 1b). To determine whether the increase in the melanin content induced by 2-BP occurred when melanocytes were cultured without KCs, normal human epidermal melanocytes (NHEMs) (Figure 1c) and HM3KO cells from a human malignant melanoma cell line (Figure 1d) were incubated with 2-BP. In both cells, 2-BP treatment increased the amount of melanin per cell in a dose-dependent manner without cytotoxicity, as determined using the thiazolyl blue tetrazolium bromide assay. Macroscopic views of cell pellets (Figure 1c and d) revealed a darker appearance of the 2-BP-treated cells than in the control cells.

Tyrosinase palmitoylation at Cys⁵⁰⁰ and its inhibition increase tyrosinase protein levels

We examined tyrosinase palmitoylation in HM3KO cells using the acyl-RAC method (resin-assisted capture of fatty-acylated proteins). The thioester bond of protein palmitoylation was

cleaved with hydroxylamine (HA), and the resultant free thiol was coupled to thiopropyl-sepharose for pulldown and subsequent immunoblotting analysis. This method directly assesses the presence of S-palmitoylation on target proteins, and omitting HA provides a control for false positives. Tyrosinase palmitoylation was significantly diminished by 2-BP for 48 hours, whereas its treatment increased total tyrosinase levels (Figure 2a–c). Palmitoylation of tyrosinase and inhibition by 2-BP were also confirmed by metabolic labeling with the ω -alkynyl-palmitate analog 17-octadecynoic acid, followed by bio-orthogonal click chemistry with azide-PEG3-biotin (Figure 2d and e). These results indicate that human tyrosinase is palmitoylated under intact culture conditions. To identify the specific palmitoylated Cys residues in human tyrosinase, MNT-1 cells were transfected with halo-tagged wild-type (WT) or mutant tyrosinase harboring C8A, C35A, or C500A mutations. These putative palmitoylated sites were screened using CSS-Palm, version 4.0 (<http://csspalm.biocuckoo.org/down.php>), a palmitoylation site prediction software. Seventy-two hours after transfection, palmitoylated tyrosinase was analyzed using an acyl-RAC assay. A significant amount of Halo-tagged tyrosinase was detected in WT, C8A, and C35A but not in C500A, tyrosinase-transfected cells (Figure 2f), indicating that Cys⁵⁰⁰ is a specific palmitoylation site in human tyrosinase. Next, NHEMs were incubated with 2-BP for 24 hours, and the total tyrosinase and palmitoylated tyrosinase protein levels were determined using the acyl-RAC assay. Although 2-BP treatment increased total tyrosinase levels in a dose-dependent manner, palmitoylated tyrosinase levels were not increased, which decreased the palmitoylated tyrosinase/total tyrosinase ratio (Figure 2g–i). Thus, the 2-BP–induced increase in melanin content was due to an increase in tyrosinase protein levels.

Palmitoylation inhibition suppresses tyrosinase degradation

To elucidate the mechanisms underlying the 2-BP–induced increase in tyrosinase protein levels, we examined the effects of tyrosinase palmitoylation on its mRNA synthesis, glycosylation, and degradation. The 2-BP–treated NHEMs showed slightly decreased tyrosinase mRNA levels (Figure 3a), suggesting that inhibition of palmitoylation affects tyrosinase protein levels through post-transcriptional events. Next, we examined whether palmitoylation affects the glycosylation modification of tyrosinase because abnormal tyrosinase glycosylation reportedly affects its stability and trafficking (Nakamura et al., 2003). Immunoblotting of tyrosinase with or without endoglycosidase H (endo H) digestion was performed using NHEM extracts pretreated with 2-BP for 24 hours. Endo H–mediated digestion generated a band of approximately 55 kDa (Figure 3b). Because this enzyme removes carbohydrate residues from N-linked glycoproteins in immature tyrosinase, the appearance of the endo H–sensitive 55 kDa band represents the presence of tyrosinase that had not been processed beyond the ER. Furthermore, 2-BP treatment did not affect the proportion of endo H–sensitive or –resistant tyrosinase, indicating that 2-BP did not influence tyrosinase glycosylation. Finally, we determined whether palmitoylation alters tyrosinase degradation. HM3KO cells were pretreated with or without 2-BP for 48 hours and treated with cycloheximide for 0.5–4 hours. The 2-BP treatment stabilized tyrosinase, and tyrosinase degradation was almost negligible during the 4-hour treatment of

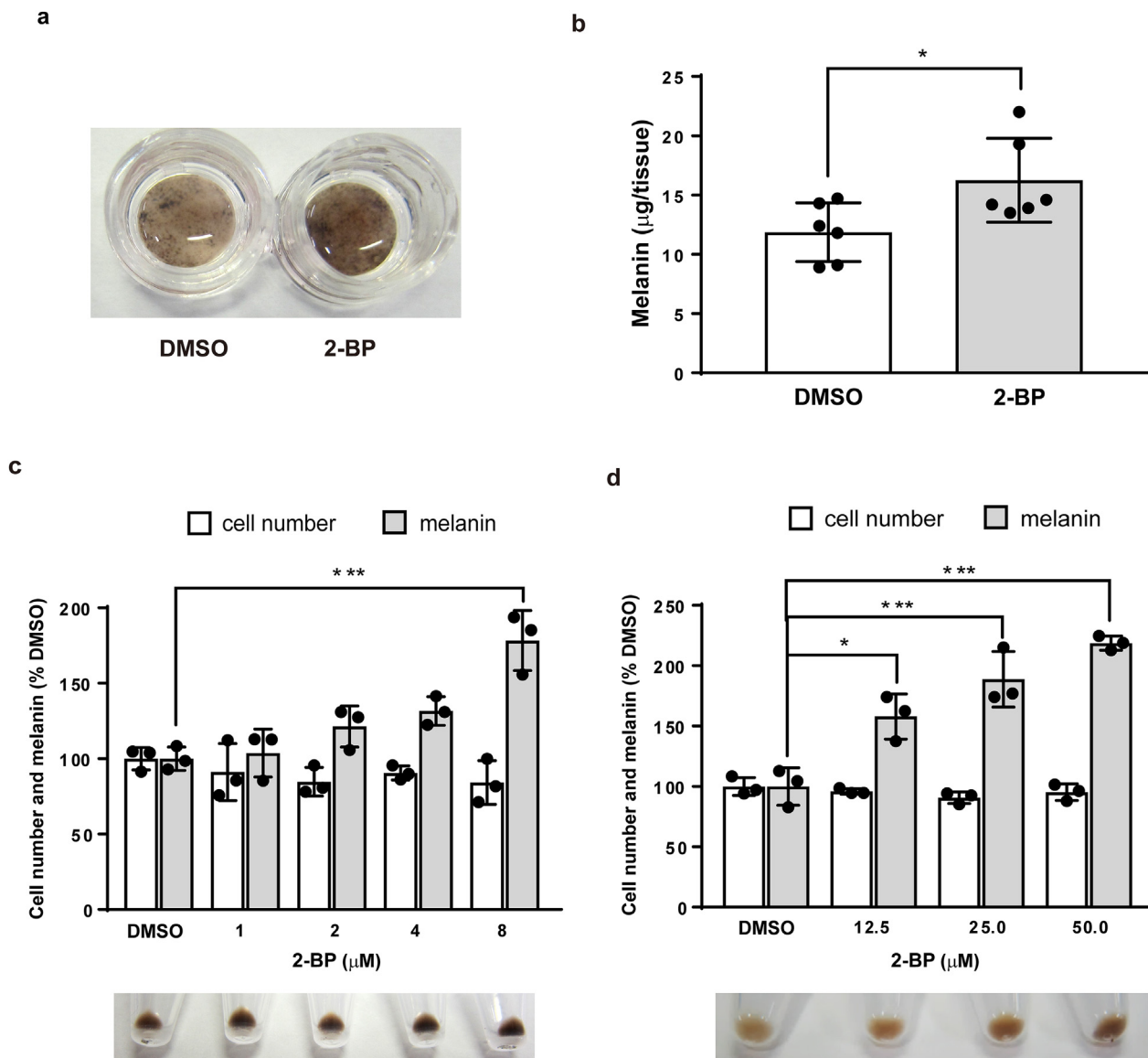


Figure 1. Effects of palmitoylation inhibitor, 2-BP, on melanin synthesis in a reconstructed human skin model and melanocytes. (a, b) Reconstructed human skin models were incubated with or without 25 μM 2-BP for 17 days. (a) Macroscopic views. (b) Melanin content. $n = 6$; $*P = 0.0321$. Analysis was performed by Student's *t*-test. (c) NHEMs and (d) HM3KO cells were treated with indicated concentrations of 2-BP for 48 and 72 hours, respectively. Cell number and melanin content were determined. $n = 3$. (c) $***P = 0.0003$. (d) $*P = 0.013$, $***P = 0.0009$ (25 μM), and $***P = 0.0001$ (50 μM). Analysis was performed by one-way ANOVA with Turkey's posthoc test. Macroscopic views of 2-BP-treated NHEM and HM3KO cell pellets are shown. 2-BP, 2-bromopalmitate; NHEM, normal human epidermal melanocyte.

cycloheximide, whereas the degradation rate in the control cells was faster than that in the 2-BP-treated cells (the half-life was 1.51 hours) (Figure 3c and d).

Nonpalmitoylated C500A mutant is highly stable compared with WT tyrosinase

We examined the stability of the C500A mutant of tyrosinase. HA-tagged WT and C500A tyrosinases plasmids were transfected and treated with cycloheximide, and the half-life of tyrosinases was determined. The half-life of WT and C500A was 1.33 and 2.51 hours, respectively (Figure 3e and f). Because tyrosinase degradation is regulated by the ubiquitin/proteasome system (Ando et al., 2006; Kageyama et al., 2004), coimmunoprecipitation experiments using overexpressed FLAG-tagged tyrosinase and HA-tagged ubiquitin were performed. Ubiquitination was strongly detected in WT compared that in C500A tyrosinase

(Figure 3g). These results imply that nonpalmitoylated tyrosinase has higher stability than the palmitoylated form and that palmitoylation of tyrosinase at Cys⁵⁰⁰ promotes its ubiquitination and degradation.

Screening of specific DHCs for tyrosinase palmitoylation

To identify the enzymes involved in tyrosinase palmitoylation, we screened 23 different palmitoyl acyl transferase DHCs. Human embryonic kidney 293T cells were transfected with each DHC subtype together with tyrosinase, and palmitoylated tyrosinase content was assessed through metabolic labeling with [³H]-palmitate. The upper and lower panels of Figure 4a show the total tyrosinase expression determined using immunoblotting and [³H]-palmitate-incorporated tyrosinase analyzed through autoradiography, respectively. [³H]-Palmitate-incorporated tyrosinases were detected in cells

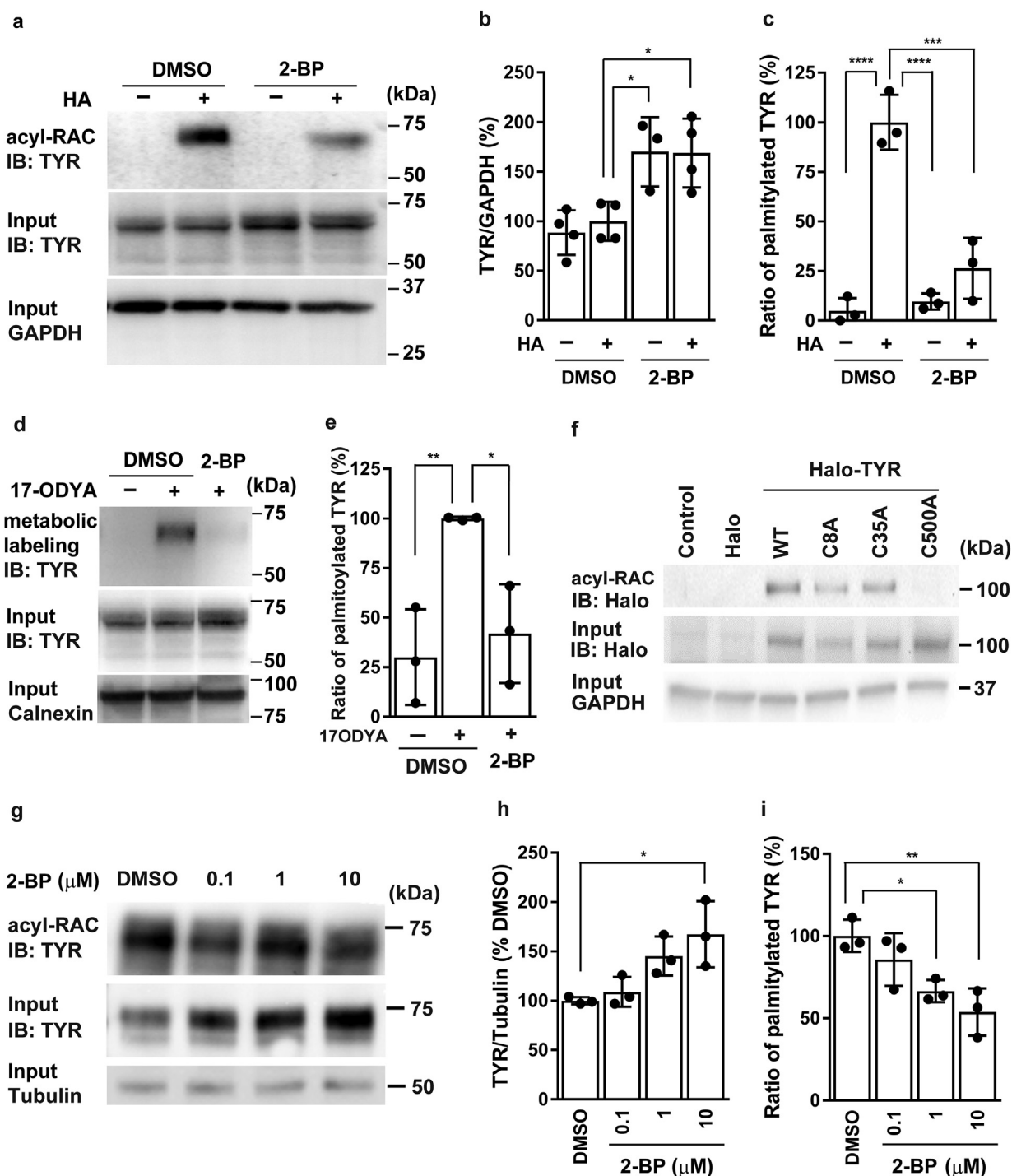


Figure 2. TYR palmitoylation and 2-BP effects. (a–c) HM3KO cells were incubated with 2-BP (50 μM, 48 hours) and subjected to (a) acyl-RAC with/without HA. (b) Total TYR normalized using GAPDH, * $P = 0.0199$ (HA[–]/2BP) and * $P = 0.0141$ (HA[+]/2BP) ($n = 4$), and (c) ratio of palmitoylated TYR (** $P = 0.0001$ and **** $P < 0.0001$, $n = 3$) are graphed. (d–e) HM3KO cells were incubated with 17-ODYA with 2-BP (50 μM, 48 hours) and (d) subjected to bio-orthogonal click chemistry. (e) Ratio of palmitoylated TYR is graphed, * $P = 0.0212$ and ** $P = 0.0093$; $n = 3$. (f) After transfection (72 hours) with Halo-tagged WT, C8A, C35A, or C500A TYR and MNT-1 cells were subjected to acyl-RAC. (g–i) NHEMs were incubated with 2-BP (0.1–10 μM, 24 hours), (g) followed by acyl-RAC. (h) TYR normalized using tubulin (* $P = 0.0183$) and (i) ratio of palmitoylated TYR (* $P = 0.0406$ and ** $P = 0.0074$, $n = 3$) are graphed. Analysis was performed by one-way ANOVA with Turkey’s posthoc test. 17-ODYA, 17-octadecynoic acid; 2-BP, 2-bromopalmitate; HA, hydroxylamine; IB, immunoblotting; NHEM, normal human epidermal melanocyte; TYR, tyrosinase; WT, wild-type.

cotransfected with DHHC3, DHHC7, or DHHC15, suggesting their involvement in tyrosinase palmitoylation. Because DHHC2 and DHHC15 are categorized as a DHHC subfamily in the phylogenetic tree (Supplementary Figure S1b) (Korycka et al.,

2012), further experiments examined DHHC2 as well. The expression of these four DHHCs in pigment cells (both NHEMs and HM3KO) was confirmed through semiquantitative RT-PCR (Supplementary Figure S1c).

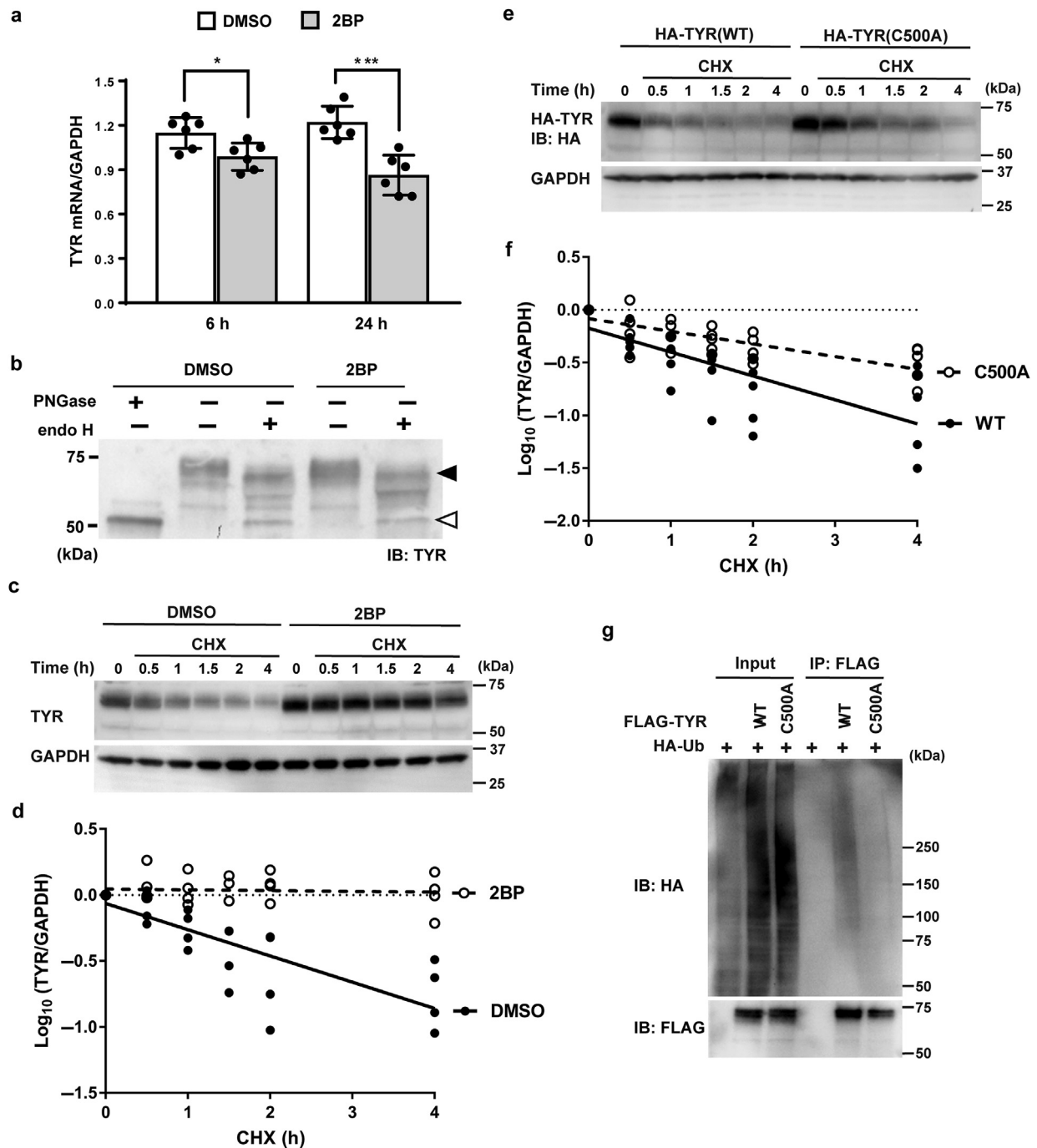


Figure 3. Palmitoylation effects on TYR mRNA, glycosylation, and degradation. (a) NHEMs were incubated with 2-BP, and TYR mRNA was analyzed through RT-qPCR and normalized using GAPDH. $n = 6$. $*P = 0.0182$ and $***P = 0.0005$. Analysis was performed by Student's t -test. (b) NHEMs were incubated with 2-BP (72 hours), and lysates were treated with endo H. Arrow and arrowhead indicate immature and mature TYR, respectively. (c, d) HM3KO cells, incubated with 2-BP (48 hours) and CHX, were subjected to immunoblotting; $n = 4$. (e, f) HA-tagged WT or nonpalmitoylatable C500A TYR-transfected HM3KO cells (48 hours) were incubated with CHX. $n = 5$. TYR band intensities were normalized using GAPDH. The intensity data were fit to linear regression to calculate the degradation rate constant used to determine the half-life. (g) HA-tagged Ub was co-overexpressed with FLAG-tagged TYR in HM3KO cells (48 hours) for immunoprecipitation to detect ubiquitination. $n = 4$. 2-BP, 2-bromopalmitate; CHX, cycloheximide; endo H, endoglycosidase H; HA, human influenza hemagglutinin; IB, immunoblotting; NHEM, normal human epidermal melanocyte; Ub, ubiquitin; TYR, tyrosinase; WT, wild-type.

Palmitoylation decreases tyrosinase level and melanin content

To examine the involvement of DHHC2, 15, 3, and 7 in tyrosinase palmitoylation and the role of tyrosinase palmitoylation in the regulation of melanin synthesis, we analyzed tyrosinase and melanin levels using HM3KO cells with stable

expression of Myc-tagged DHHC2, 15, 3, or 7 (Figure 4b). Melanin content was significantly lower in cells stably expressing DHHC2, 15, and 3 but not DHHC7 than in stable Myc vector-expressing control cells (Figure 4c). In addition, tyrosinase protein levels were lower in cells stably expressing DHHC2, 15, 3, and 7 (Figure 4d). These results suggest that

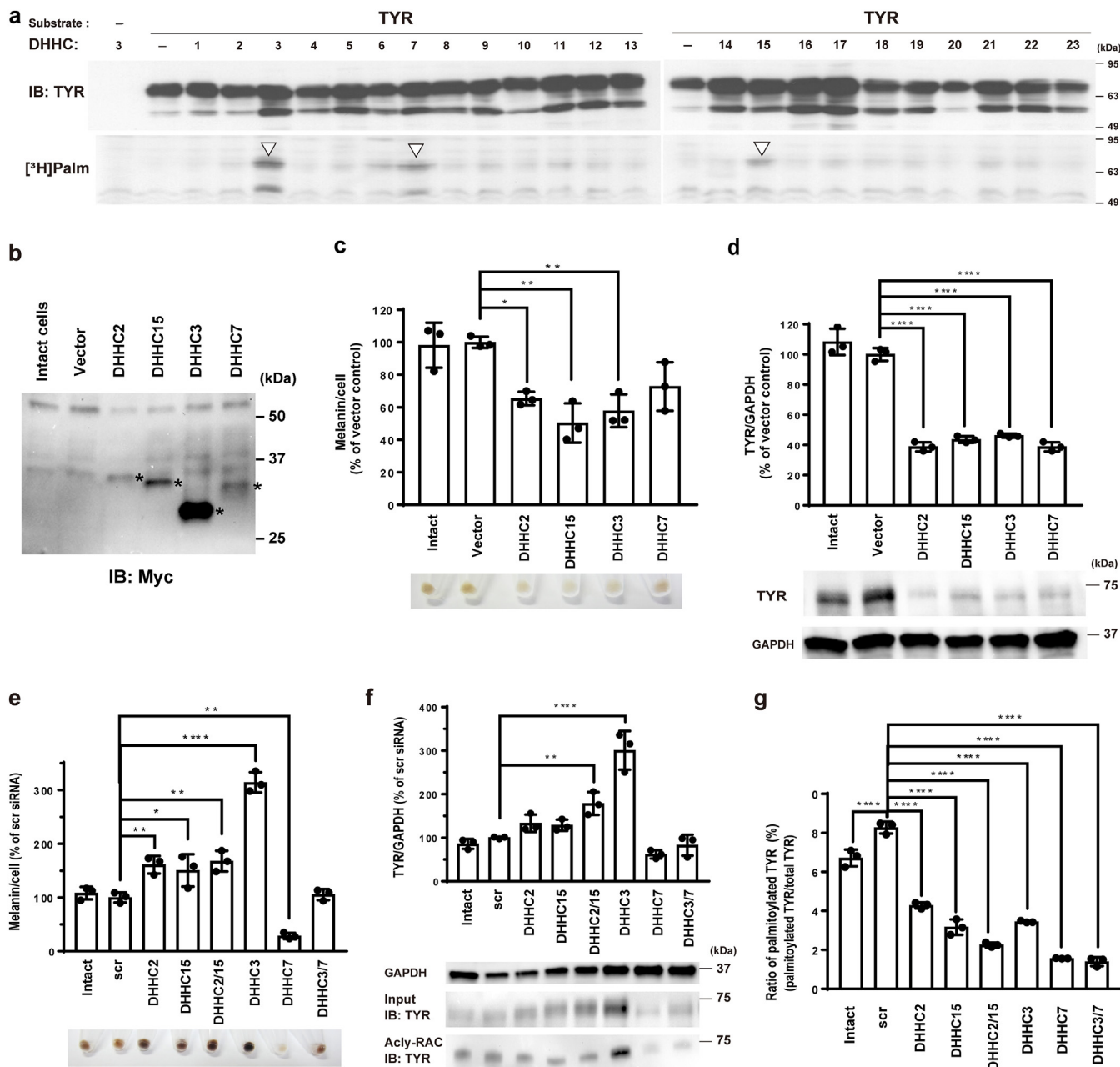


Figure 4. DHCs effects on melanin, TYR, and palmitoylated TYR. (a) HEK293T cells were transfected with TYR and DHC plasmids. After metabolic labeling (³H-palmitate), SDS-PAGE-separated proteins were subjected to immunoblotting and autoradiography (lower, arrowheads: palmitoylated TYR). (b–d) Stable Myc-tagged DHC expression (*) in HM3KO cells confirmed using immunoblotting. (b) Equal amounts of the proteins were loaded. Melanin content in the stable HM3KO cells is shown. (c) **P* = 0.0186 (DHC2), ***P* = 0.0011 (DHC15), and ***P* = 0.0044 (DHC3). TYR levels in the stable HM3KO cells are shown. TYR band intensities were normalized using GAPDH. (d) *****P* < 0.0001. *n* = 3. (e–g) Melanin content in HM3KO cells 3 days after DHC siRNA transfection. (e) **DHC2, *DHC15, **DHC2/15, ****DHC3, **DHC7. Total TYR levels were normalized using GAPDH. (f) *DHC2/15 and ****DHC3. Palmitoylated TYR/total TYR is shown. *****P* < 0.0001. (g) Analysis was performed with one-way ANOVA with Turkey’s test. *n* = 3. DHC, Asp-His-His-Cys; HEK293T, human embryonic kidney 293T, IB, immunoblotting; scr, scramble siRNA, small interfering RNA; TYR, tyrosinase.

DHC2, 15, 3, and 7 induced palmitoylation-mediated tyrosinase level decrease in melanogenic cells and that tyrosinase palmitoylation by these DHCs, excluding DHC7, resulted in decreased melanin content.

DHC2, 15, and 3 depletion increases tyrosinase levels and melanin content

To further investigate the role of tyrosinase palmitoylation in the regulation of melanin synthesis, we knocked down

DHC2, 15, 3, and 7 in HM3KO cells using respective small interfering RNAs (siRNAs). Three days after transfection with siRNAs against DHC2, 3, 7, or 15, the knockdown effect of each siRNA was confirmed using qPCR (Supplementary Figure S2a–d). These four DHC siRNAs had no significant effect on tyrosinase mRNA levels (Supplementary Figure S2e). Knockdown of DHC2, 15, or 3 and double knockdown of DHC2 and 15 increased melanin content and tyrosinase levels (Figure 4e and f). The cell pellet color became darker by

the knockdown of DHHC2, 15, or 3 (Figure 4e). These effects were most profound by DHHC3 knockdown; however, knockdown of DHHC7 decreased melanin content and tyrosinase levels (Figure 4e and f). The ratio of palmitoylated tyrosinase/total tyrosinase was lower in cells with knockdown of DHHC2, 15, 2/15, 3, 7, or 3/7 than in control siRNA-transfected cells (Figure 4g). These results indicate that the inhibition of tyrosinase palmitoylation elevated tyrosinase protein levels, which increased melanin synthesis. DHHC7 showed palmitoyl transferase activity on tyrosinase (Figure 4a and g) but did not produce a tyrosinase-mediated melanin increase, at least in HM3KO cells (Figure 4e–g).

Intracellular localization of DHHC2, 15, and 3

To study the intracellular localization of DHHC2, 15, and 3 in NHEMs, N-terminally tagged (His₆ and Myc) proteins were overexpressed in NHEMs. Only DHHC2 merged with HMB45, a melanosome marker that recognizes PMEL17/gp100 in stage II melanosomes (Figure 5a and Supplementary Figure S3). DHHC2 and 3 colocalized with calnexin, an ER marker (Figure 5b and Supplementary Figure S3). DHHC3 and 15 mainly colocalized with GM130, a *cis*-Golgi apparatus marker (Figure 5c and Supplementary Figure S3). In contrast, DHHC2 colocalized with Vti1b, a *cis*/medial/*trans*-Golgi apparatus marker (Figure 5d and Supplementary Figure S3). Next, we examined the colocalization of these DHHCs with tyrosinase. All DHHCs were colocalized with tyrosinase in the perinuclear area; however, only DHHC2 was colocalized with tyrosinase at the cytosolic puncta (Figure 6a). These results (Figure 6b) suggest that DHHC2, 15, and 3 palmitoylate tyrosinase in the ER, Golgi apparatus, and/or melanosomes and that only DHHC2 functions in melanosomes. Coimmunoprecipitation using overexpressed FLAG-tagged tyrosinase and Myc-tagged DHHC (2 or 3) in COS-7 cells showed (i) coexpression of DHHC-induced appearance of the immature tyrosinase at 55–60 kDa through an unknown mechanism; (ii) that although expression levels between DHHC2 and DHHC3 were not similarly consistent with a previous report (Ohno et al., 2006), DHHC2 binds to both mature and immature tyrosinase, whereas DHHC3 predominantly binds to immature tyrosinase; and (iii) that both DHHC2 and DHHC3 predominantly bind to WT compared with binding to C500A-mutant tyrosinase (Figure 6c).

DISCUSSION

More than 150 genes are involved in melanogenesis (Yamaguchi and Hearing, 2014). Although palmitoylation involvement in melanogenesis in *Aspergillus* (Upadhyay et al., 2016) and palmitoylation of melanocortin-1 receptor (MC1R) in humans (Chen et al., 2017) have been reported, in this study, we showed palmitoylation of tyrosinase—the rate-limiting enzyme—in melanogenesis.

In the human skin, melanin synthesis in melanocytes is regulated by physiological factors from KCs, including α -melanocyte-stimulating hormone (α -MSH), adrenocorticotropic hormone (ACTH), and endothelin-1 (Yamaguchi and Hearing, 2014). In this study, inhibition of tyrosinase palmitoylation increased melanin content in a human skin model consisting of KCs and melanocytes as well as cultured melanocytes, suggesting that palmitoylation inhibition increased melanin synthesis, not through paracrine factors from KCs. Cys⁵⁰⁰ in the

C-terminal cytoplasmic tail of tyrosinase, which includes approximately 30 amino acids (Lai et al., 2018), is well-conserved in mammals. Although consensus amino acid sequences for palmitoylation remain unknown, Cys residues in the juxta-transmembrane region of the C-terminal cytoplasmic tail of membrane proteins have been reported as palmitoylation-target sites (Blaskovic et al., 2013; Fukata and Fukata, 2010).

The intracellular distribution of endogenous DHHC family proteins remains unclear because they are expressed at low levels (Zaballa and van der Goot, 2018). In this study, transiently overexpressed DHHC2, 15, and 3 were localized in the ER and/or Golgi apparatus in NHEMs. This intracellular distribution was consistent with a previous report using human embryonic kidney 293T cells (Ohno et al., 2006). Notably, DHHC2 was localized in melanosomes. Melanosomes are classified into four stages (I–IV) on the basis of their morphology and maturation. Tyrosinase is transferred to stage II melanosomes through endosomes, where it initiates melanin synthesis (Ohbayashi and Fukuda, 2020). Adapter protein-1 (AP-1) and adapter protein-3 (AP-3) are involved in tyrosinase sorting from endosomes to melanosomes (Theos et al., 2005) and recognize melanosome sorting signals (with the consensus motif [D/E]xxxL[L/I]) with different affinities (Bonifacino and Traub, 2003; Theos et al., 2005), subsequently sorting tyrosinase to distinct destinations. Tyrosinase has the amino acid sequence ⁵⁰⁹E EKQPLL⁵¹⁵ in its C-terminal cytoplasmic tail (Höning et al., 1998). Interestingly, tyrosinase is sorted to the plasma membrane and not to melanosomes in platinum mice, with truncated 27 amino acids in the C-terminal cytoplasmic tail (Beermann et al., 1995; Vijayasaradhi et al., 1995). DHHC2 has a similar amino acid sequence, ³³⁰ESQSHLL³³⁶, in its C-terminal region, which may function as a melanosome-targeting signal. DHHC3 and DHHC7 are the closest homologs in DHHC proteins (Korycka et al., 2012) and are ubiquitously expressed in many tissues (Ohno et al., 2006), whereas DHHC2 and DHHC15 are expressed in specific tissues (Ohno et al., 2006). Moreover, DHHC 3 and DHHC7 have broad substrate specificity (Fukata et al., 2006) owing to their PDZ domains in the C-terminus (Malgapo and Linder, 2021). We propose that DHHC2 may palmitoylate tyrosinase in the ER, Golgi apparatus, and melanosomes. DHHC2 palmitoylates tyrosinase at all the three sites, only melanosomes, or at a few sites. Notably, we did not detect DHHC2 activity for tyrosinase palmitoylation in human embryonic kidney 293T cells, suggesting that DHHC2 functions as a palmitoylation enzyme only in melanosomes. Moreover, the Golgi-localized DHHC proteins, such as DHHC15 and DHHC3, may mainly function in the delivery of the newly synthesized tyrosinase. Indeed, coimmunoprecipitation results showed that DHHC2 and DHHC3 dominantly bind to mature and immature tyrosinase, respectively (Figure 6c).

Supplementary Figure S4 shows a model summarizing this study on the regulation of tyrosinase and melanin synthesis. Tyrosinase is synthesized in the ER, matured in the Golgi apparatus, and finally trafficked to melanosomes through endosomes. In this process, tyrosinase may be palmitoylated in the ER by DHHC2 and DHHC3, in the Golgi apparatus by DHHC2, DHHC15, and DHHC3, and in melanosomes by DHHC2. Thus, the induction of tyrosinase palmitoylation accelerates the downregulation of tyrosinase protein levels and melanogenesis. Conversely, inhibition of tyrosinase

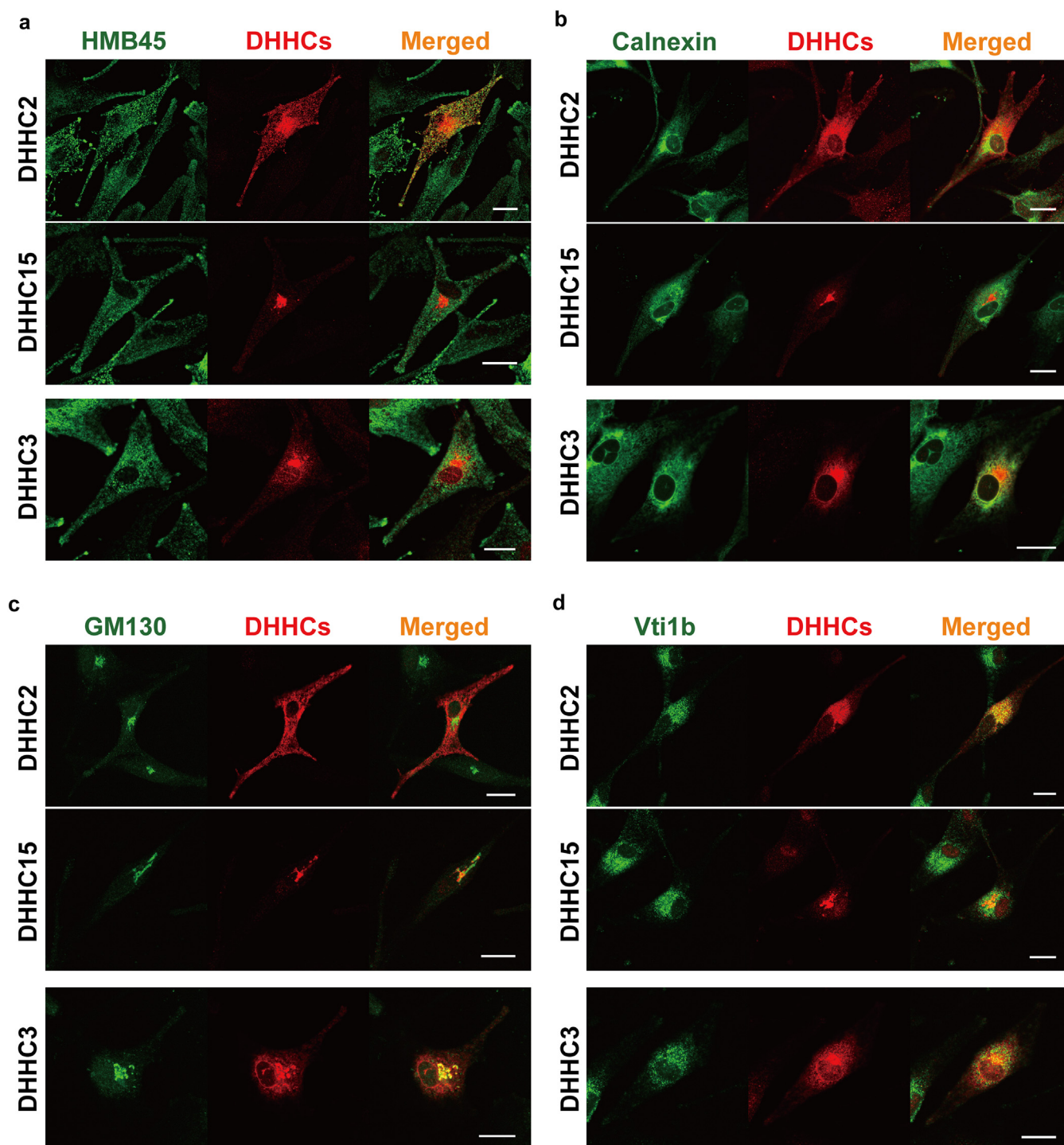


Figure 5. Intercellular localization of DHHC2, DHHC15, and DHHC3 in NHEMs. NHEMs were transfected with plasmid encoding Myc-tagged DHHC2, DHHC15, or DHHC3. Two days after transfection, they were fixed, permeabilized, and stained with (a) HMB45, (b) calnexin, (c) GM130, or (d) Vti1b antibody and a Myc antibody. Bar = 20 μ m. DHHC, Asp-His-His-Cys; NHEM, normal human epidermal melanocyte.

palmitoylation upregulates melanogenesis. Indeed, ubiquitination was more dominant in WT than in the C500A-mutant tyrosinase (Figure 3g). The degradation of palmitoylated tyrosinase by DHHC2 on melanosomes may occur in the Rab7B/LAMP1-positive endosomes in transferred KCs (Fukuda, 2021; Marubashi and Fukuda, 2020).

The ubiquitination of tyrosinase regulates melanin synthesis (Ando et al., 2006; Kageyama et al., 2004). p38 MAPK is

involved in melanogenesis induced by α -MSH (Smalley and Eisen, 2000) and UV irradiation (Galibert et al., 2001), and knockdown of p38 MAPK enhances tyrosinase expression through decreased ubiquitination, thereby stimulating melanogenesis (Bellei et al., 2010). Hence, melanogenic stimuli (α -MSH and UV) have regulatory effects on tyrosinase levels. Ubiquitination sites in tyrosinase have not yet been identified; however, there are two candidate lysines (Lys⁵¹⁰ and Lys⁵¹⁷) in

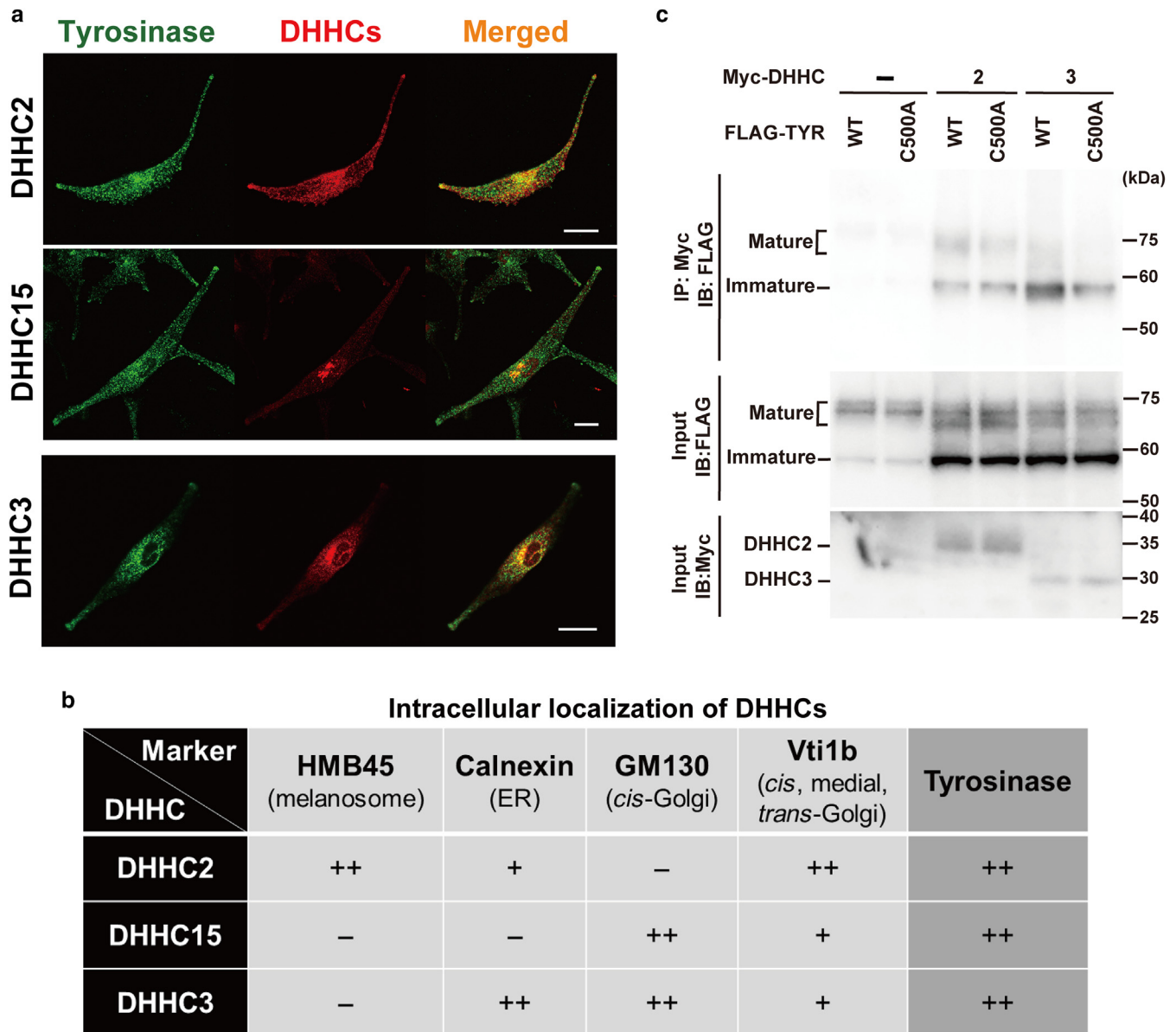


Figure 6. Colocalization and binding between DHHC and tyrosinase. (a) NHEMs were transfected with plasmid encoding Myc-tagged DHHC2, DHHC15, or DHHC3. Two days after transfection, they were fixed, permeabilized, and stained with antibodies against tyrosinase and Myc. Bar = 20 μ m. (b) Intracellular localization of DHHCs (shown in Figure 5) and colocalization of DHHCs and tyrosinase (shown in Figure 6a) are summarized. (c) COS-7 cells were cotransfected with plasmids encoding FLAG-tagged tyrosinase (WT or C500A mutant) and Myc-tagged DHHC (DHHC2 or DHHC3). Two days after transfection, cells were lysed and immunoprecipitated using a magnetic agarose-conjugated Myc antibody, followed by immunoblotting with an HRP-conjugated FLAG antibody. Comparable input of tyrosinase and DHHC were confirmed using HRP-conjugated FLAG and Myc antibodies, respectively. n = 4. DHHC, Asp-His-His-Cys; HRP, horseradish peroxidase; IB, immunoblotting; NHEM, normal human epidermal melanocyte; WT, wild-type.

the C-terminal cytoplasmic tail (UbPred: predictor of protein ubiquitination). We assumed that conformational changes in the cytoplasmic tail and/or palmitoylation-mediated alterations in the subcellular localization of tyrosinase induce its ubiquitination. However, the synergistic effects of palmitoylation and other post-transcriptional modifications in tyrosinase remain unclear.

In conclusion, pigmentation in the human skin shows notable diversity among Caucasians, Asians, and Africans. Our findings indicate that the palmitoylation-induced degradation of tyrosinase is a critical regulator and modulator of melanogenesis. However, interactions and cross-talk among modifications, such as palmitoylation and

ubiquitination, remain unclear. Further studies are required to examine the effects of palmitoylation on other modifications of melanogenesis.

MATERIALS AND METHODS

The detailed materials and methods are provided in the Supplementary Materials and Methods. This study, using commercially available human materials, was approved by the Committee for Safe Handling of Living Modified Organisms at Kobe University (Kobe, Japan).

Cells

HM3KO (RRID:CVCL_5620) and MNT-1 (RRID:CVCL_5624) human melanoma cells, NHEMs (moderate pigmentation, Kurabo Industries,

Osaka, Japan), and a three-dimensional reconstructed human skin model (MEL-300-A, Kurabo Industries) were used.

Plasmids, siRNAs, and transfection

The pCE-puro His₆-Myc-DHHC plasmids were a kind gift from Akio Kihara (Hokkaido University, Sapporo, Japan) (Ohno et al., 2006). Human tyrosinase (*hTYR*) in BCMGS NHT2 plasmid has been previously reported (Tsuboi et al., 1998).

The 2-BP effect on melanin synthesis and growth in NHEMs and HM3KO cells

NHEMs and HM3KO cells were treated with 2-BP (Sigma-Aldrich, St. Louis, MO) for 24–48 hours and 48–72 hours, respectively. Cells were washed with Dulbecco's PBS(–) and ethanol-ether 1:1 (v/v) to remove opaque substances other than melanin. After discarding the organic solvent, the dried cells were solubilized in 1 M sodium hydrate containing 10% DMSO by incubation at 80 °C for 10 minutes. The absorbance of dissolved melanin at 490 nm was measured using a microplate reader (Bio-Rad Laboratories, Hercules, CA). Protein concentration in the cell lysates was determined using a BCA protein assay kit (Thermo Fisher Scientific, Waltham, CA). The ratio of absorbance₄₉₀ to protein content was used to compare intracellular melanin content.

The 2-BP effect on melanin synthesis and cytotoxicity in the human skin model

Dulbecco's PBS(–) containing 0.01% DMSO or 25 μM 2-BP (50 μl) was applied to the surface of the skin model. The tissues were then incubated for 17 days. The culture medium (long-life maintenance medium) and test solution were changed every other day. Eumelanin content was analyzed by alkaline hydrogen peroxide oxidation to detect pyrrole-2, 3, 5,-tricarboxylic acid (Ito et al., 2011), and pheomelanin content was analyzed through hydriodic acid hydrolysis and high-performance liquid chromatography assay to detect 4-amino-3-hydroxyphenylalanine (Wakamatsu et al., 2006). Cell viability was determined using a thiazolyl blue tetrazolium bromide assay kit (Kurabo Industries).

Detection of palmitoylated tyrosinase

Palmitoylated tyrosinase was detected using acyl-RAC assay (Forrester et al., 2011) or metabolic labeling and click chemistry (Martin and Cravatt, 2009).

Screening for tyrosinase-specific DHHCs

Systematic screening for tyrosinase-specific DHHCs was performed as previously reported (Fukata et al., 2006).

Immunoblotting and immunoprecipitation

Cells were solubilized in a cell lysis buffer (50 mM Tris/hydrogen chloride [pH 7.4], 150 mM sodium chloride, 5 mM EDTA, 10% glycerol, 1% NP-40, and a protease inhibitor cocktail). After centrifugation, the protein concentrations of the cell lysates were determined and then used for each experiment.

Endoglycosidase H digestion

NHEMs were seeded at a density of 2×10^5 cells per 25 cm² flask. The medium was changed to that containing 5.0 μM 2-BP. After 72-hour treatment, 3 μg of protein from the cell extracts were digested with 1,000 units of Endo H (New England BioLabs, Ipswich, MA) for 3 hours at 37 °C, and tyrosinase proteins were analyzed by immunoblotting.

Tyrosinase degradation assay

HM3KO cells were seeded at a density of 1.5×10^5 cells/12-well plate and treated with a medium containing 50 μM 2-BP and 1.0 μg/ml cycloheximide. In the case of transfected experiments

(HA-tagged *hTYR* plasmids), cells were treated with a medium containing 1.0 μg/ml cycloheximide. After cycloheximide treatment, the cells were solubilized in the lysis buffer, and tyrosinase proteins were analyzed using immunoblotting.

Immunofluorescence microscopy

Two days after transfection, the cells were fixed with 4% paraformaldehyde, permeabilized with 0.1% Triton X-100 in PBS(–) for 15 minutes, and then stained with primary antibodies and CF488A or Alexa Fluor 594–conjugated secondary antibodies. Labeled cells were observed using an LSM 700 laser scanning confocal microscope (Carl Zeiss, Oberkochen, Germany).

Data Availability Statement

Data supporting the findings of this study are available in the supplementary materials of this article.

ORCIDiDs

Yoko Niki: <http://orcid.org/0000-0003-0391-6631>
 Naoko Adachi: <http://orcid.org/0000-0002-8797-0717>
 Masaki Fukata: <http://orcid.org/0000-0001-5200-9806>
 Yuko Fukata: <http://orcid.org/0000-0001-7724-8643>
 Shinichiro Oku: <http://orcid.org/0000-0002-1916-1870>
 Chieko Makino-Okamura: <http://orcid.org/0000-0001-7074-1494>
 Seiji Takeuchi: <http://orcid.org/0000-0003-4741-3382>
 Kazumasa Wakamatsu: <http://orcid.org/0000-0003-1748-9001>
 Shosuke Ito: <http://orcid.org/0000-0001-9182-5144>
 Lieve Declercq: <http://orcid.org/0000-0003-3693-5118>
 Daniel B. Yarosh: <http://orcid.org/0000-0002-0786-5985>
 Tomas Mammone: <http://orcid.org/0000-0002-5255-5951>
 Chikako Nishigori: <http://orcid.org/0000-0002-6784-2849>
 Naoaki Saito: <http://orcid.org/0000-0003-3389-1367>
 Takehiko Ueyama: <http://orcid.org/0000-0002-5647-3937>

CONFLICT OF INTEREST

Part of this study was funded by the Estée Lauder Companies. LD and DBY were employees of the Estée Lauder Companies and supervised this study.

ACKNOWLEDGMENTS

This study was supported by grants from the joint research program of the Biosignal Research Center, Kobe University (202008 to YN); Grant-in-Aid for Human Resource Development Program for Science and Technology from the Ministry of Education, Culture, Sports, Science and Technology, which was obtained by the Kobe University Gender Equality Office (to NA); and the Japan Society for the Promotion of Science KAKENHI (16KK0181 and JP22K06858 to NA and JP21H02672 to TU).

AUTHOR CONTRIBUTIONS

Conceptualization: YN, LD, DBY, TM, CN, NS; Formal Analysis: YN, NA, TU; Investigations: YN, NA, MF, YF, SO, CMO, ST, TU; Funding Acquisition: YN, NS, NA, TU; Validation: YN, NA, KW, SI, CN, NS, TU; Visualization: YN, NA, MF, YF, SO, TU. Writing – Original Draft Preparation: YN, TU. Writing – Review and Editing: YN, NA, MF, YF, SO, CMO, ST, KW, SI, LD, DBY, TM, CN, NS, TU

SUPPLEMENTARY MATERIAL

Supplementary material is linked to the online version of the paper at www.jidonline.org, and at <https://doi.org/10.1016/j.jid.2022.08.040>

REFERENCES

- Ando H, Ichihashi M, Hearing VJ. Role of the ubiquitin proteasome system in regulating skin pigmentation. *Int J Mol Sci* 2009;10:4428–34.
- Ando H, Niki Y, Ito M, Akiyama K, Matsui MS, Yarosh DB, et al. Melanosomes are transferred from melanocytes to keratinocytes through the processes of packaging, release, uptake, and dispersion. *J Invest Dermatol* 2012;132:1222–9.
- Ando H, Wen ZM, Kim HY, Valencia JC, Costin GE, Watabe H, et al. Intracellular composition of fatty acid affects the processing and function of tyrosinase through the ubiquitin-proteasome pathway. *Biochem J* 2006;394:43–50.
- Beermann F, Orlov SJ, Boissy RE, Schmidt A, Boissy YL, Lamoreux ML. Misrouting of tyrosinase with a truncated cytoplasmic tail as a result of the murine platinum (cp) mutation. *Exp Eye Res* 1995;61:599–607.

- Bellei B, Maresca V, Flori E, Pitisci A, Larue L, Picardo M. p38 regulates pigmentation via proteasomal degradation of tyrosinase. *J Biol Chem* 2010;285:7288–99.
- Blaskovic S, Blanc M, van der Goot FG. What does S-palmitoylation do to membrane proteins? *FEBS J* 2013;280:2766–74.
- Bonifacino JS, Traub LM. Signals for sorting of transmembrane proteins to endosomes and lysosomes. *Annu Rev Biochem* 2003;72:395–447.
- Chamberlain LH, Shipston MJ. The physiology of protein S-acylation. *Physiol Rev* 2015;95:341–76.
- Chen S, Zhu B, Yin C, Liu W, Han C, Chen B, et al. Palmitoylation-dependent activation of MC1R prevents melanomagenesis. *Nature* 2017;549:399–403.
- Forrester MT, Hess DT, Thompson JW, Hultman R, Moseley MA, Stamler JS, et al. Site-specific analysis of protein S-acylation by resin-assisted capture. *J Lipid Res* 2011;52:393–8.
- Fujita H, Motokawa T, Katagiri T, Yokota S, Yamamoto A, Himeno M, et al. Inulavosin, a melanogenesis inhibitor, leads to mistargeting of tyrosinase to lysosomes and accelerates its degradation [published correction appears in *J Invest Dermatol* 2010;130:908]. *J Invest Dermatol* 2009;129:1489–99.
- Fukata M, Fukata Y, Adesnik H, Nicoll RA, Brecht DS. Identification of PSD-95 palmitoylating enzymes. *Neuron* 2004;44:987–96.
- Fukata Y, Fukata M. Protein palmitoylation in neuronal development and synaptic plasticity. *Nat Rev Neurosci* 2010;11:161–75.
- Fukata Y, Iwanaga T, Fukata M. Systematic screening for palmitoyl transferase activity of the DHHC protein family in mammalian cells. *Methods* 2006;40:177–82.
- Fukuda M. Rab GTPases: key players in melanosome biogenesis, transport, and transfer. *Pigment Cell Melanoma Res* 2021;34:222–35.
- Galibert MD, Carreira S, Goding CR. The Usf-1 transcription factor is a novel target for the stress-responsive p38 kinase and mediates UV-induced tyrosinase expression. *EMBO J* 2001;20:5022–31.
- Höning S, Sandoval IV, von Figura K. A di-leucine-based motif in the cytoplasmic tail of LIMP-II and tyrosinase mediates selective binding of AP-3. *EMBO J* 1998;17:1304–14.
- Ito S, Nakanishi Y, Valenzuela RK, Brilliant MH, Kolbe L, Wakamatsu K. Usefulness of alkaline hydrogen peroxide oxidation to analyze eumelanin and pheomelanin in various tissue samples: application to chemical analysis of human hair melanins. *Pigment Cell Melanoma Res* 2011;24:605–13.
- Ito S, Wakamatsu K. Chemistry of mixed melanogenesis—pivotal roles of dopaquinone. *Photochem Photobiol* 2008;84:582–92.
- Kageyama A, Oka M, Okada T, Nakamura S, Ueyama T, Saito N, et al. Down-regulation of melanogenesis by phospholipase D2 through ubiquitin proteasome-mediated degradation of tyrosinase. *J Biol Chem* 2004;279:27774–80.
- Kobayashi T, Urabe K, Winder A, Jiménez-Cervantes C, Imokawa G, Brewington T, et al. Tyrosinase related protein 1 (TRP1) functions as a DHICA oxidase in melanin biosynthesis. *EMBO J* 1994;13:5818–25.
- Korycka J, Łach A, Heger E, Bogusławska DM, Wolny M, Toporkiewicz M, et al. Human DHHC proteins: a spotlight on the hidden player of palmitoylation. *Eur J Cell Biol* 2012;91:107–17.
- Lai X, Wichers HJ, Soler-Lopez M, Dijkstra BW. Structure and function of human tyrosinase and tyrosinase-related proteins. *Chemistry* 2018;24:47–55.
- Linder ME, Deschenes RJ. Palmitoylation: policing protein stability and traffic. *Nat Rev Mol Cell Biol* 2007;8:74–84.
- Malgapo MIP, Linder ME. Substrate recruitment by zDHHC protein acyltransferases. *Open Biol* 2021;11:210026.
- Martin BR, Cravatt BF. Large-scale profiling of protein palmitoylation in mammalian cells. *Nat Methods* 2009;6:135–8.
- Martínez-Esparza M, Jiménez-Cervantes C, Beermann F, Aparicio P, Lozano JA, García-Borrón JC. Transforming growth factor-beta1 inhibits basal melanogenesis in B16/F10 mouse melanoma cells by increasing the rate of degradation of tyrosinase and tyrosinase-related protein-1. *J Biol Chem* 1997;272:3967–72.
- Martínez-Esparza M, Jiménez-Cervantes C, Solano F, Lozano JA, García-Borrón JC. Mechanisms of melanogenesis inhibition by tumor necrosis factor-alpha in B16/F10 mouse melanoma cells. *Eur J Biochem* 1998;255:139–46.
- Marubashi S, Fukuda M. Rab7B/42 is functionally involved in protein degradation on melanosomes in keratinocytes. *Cell Struct Funct* 2020;45:45–55.
- Mitchell DA, Vasudevan A, Linder ME, Deschenes RJ. Protein palmitoylation by a family of DHHC protein S-acyltransferases. *J Lipid Res* 2006;47:1118–27.
- Nakamura K, Yoshida M, Uchiwa H, Kawa Y, Mizoguchi M. Down-regulation of melanin synthesis by a biphenyl derivative and its mechanism. *Pigment Cell Res* 2003;16:494–500.
- Niki Y, Yoshida M, Ando H, Wakamatsu K, Ito S, Harada N, et al. 1-(2,4-dihydroxyphenyl)-3-(2,4-dimethoxy-3-methylphenyl)propane inhibits melanin synthesis by dual mechanisms. *J Dermatol Sci* 2011;63:115–21.
- Ohbayashi N, Fukuda M. Recent advances in understanding the molecular basis of melanogenesis in melanocytes. *F1000Res* 2020;9:F1000.
- Ohno Y, Kihara A, Sano T, Igarashi Y. Intracellular localization and tissue-specific distribution of human and yeast DHHC cysteine-rich domain-containing proteins. *Biochim Biophys Acta* 2006;1761:474–83.
- Park SH, Kim DS, Lee HK, Kwon SB, Lee S, Ryoo IJ, et al. Long-term suppression of tyrosinase by terrien via tyrosinase degradation and its decreased expression. *Exp Dermatol* 2009;18:562–6.
- Resh MD. Trafficking and signaling by fatty-acylated and prenylated proteins. *Nat Chem Biol* 2006;2:584–90.
- Serre C, Busuttill V, Botto JM. Intrinsic and extrinsic regulation of human skin melanogenesis and pigmentation. *Int J Cosmet Sci* 2018;40:328–47.
- Smalley K, Eisen T. The involvement of p38 mitogen-activated protein kinase in the alpha-melanocyte stimulating hormone (alpha-MSH)-induced melanogenic and anti-proliferative effects in B16 murine melanoma cells. *FEBS Lett* 2000;476:198–202.
- Svedine S, Wang T, Halaban R, Hebert DN. Carbohydrates act as sorting determinants in ER-associated degradation of tyrosinase. *J Cell Sci* 2004;117:2937–49.
- Theos AC, Tenza D, Martina JA, Hurbain I, Peden AA, Sviderskaya EV, et al. Functions of adaptor protein (AP)-3 and AP-1 in tyrosinase sorting from endosomes to melanosomes. *Mol Biol Cell* 2005;16:5356–72.
- Tsuboi T, Kondoh H, Hiratsuka J, Mishima Y. Enhanced melanogenesis induced by tyrosinase gene-transfer increases boron-uptake and killing effect of boron neutron capture therapy for amelanotic melanoma. *Pigment Cell Res* 1998;11:275–82.
- Tsukamoto K, Jackson IJ, Urabe K, Montague PM, Hearing VJ. A second tyrosinase-related protein, TRP-2, is a melanogenic enzyme termed dopachrome tautomerase. *EMBO J* 1992;11:519–26.
- Upadhyay S, Xu X, Lin X. Interactions between melanin enzymes and their atypical recruitment to the secretory pathway by palmitoylation. *mBio* 2016;7:e01925–16.
- Vijayaradhi S, Xu Y, Bouchard B, Houghton AN. Intracellular sorting and targeting of melanosomal membrane proteins: identification of signals for sorting of the human brown locus protein, gp75. *J Cell Biol* 1995;130:807–20.
- Wakamatsu K, Kavanagh R, Kadekaro AL, Terzieva S, Sturm RA, Leachman S, et al. Diversity of pigmentation in cultured human melanocytes is due to differences in the type as well as quantity of melanin. *Pigment Cell Res* 2006;19:154–62.
- Yamaguchi Y, Hearing VJ. Melanocytes and their diseases. *Cold Spring Harb Perspect Med* 2014;4:a017046.
- Yang W, Di Vizio D, Kirchner M, Steen H, Freeman MR. Proteome scale characterization of human S-acylated proteins in lipid raft-enriched and non-raft membranes. *Mol Cell Proteomics* 2010;9:54–70.
- Zaballa ME, van der Goot FG. The molecular era of protein S-acylation: spotlight on structure, mechanisms, and dynamics. *Crit Rev Biochem Mol Biol* 2018;53:420–51.



This work is licensed under a Creative Commons Attribution 4.0 International License. To view a copy of this license, visit <http://creativecommons.org/licenses/by/4.0/>

SUPPLEMENTARY MATERIALS AND METHODS

Chemicals and antibodies

Chemical reagents were purchased from Fujifilm Wako Pure Chemical (Osaka, Japan). Antibody against tyrosinase (T-311, sc-20035; RRID:AB_628420; 1:400 for immunoblotting [IB] and 1:1,000 for immunofluorescence [IF]) was purchased from Santa Cruz Biotechnology (Dallas, TX). Antibody against GAPDH (6C5; RRID:AB_437392; 1:10,000 for IB) was purchased from Abcam (Austin, TX). Antibodies against HMB45 (ab787; RRID:AB_306146; 1:1,000 for IF) and calnexin (ab22595; RRID:AB_2069006; 1:1,000 for IF and IB) were purchased from Abcam (Cambridge, United Kingdom); the antibodies against GM130 (M179-A48; RRID:AB_10694889; 1:100 for IF), Myc-tag (562; RRID:AB_591105; 1:2,000 for IF), Myc-tag (M047-3; RRID:AB_591112; 1:1,000 for IF), Myc-tag mAb-Magnetic Agarose (M047-10), Myc-tag mAb-horseradish peroxidase-Direct (M192-7; 1:10,000 for IB), DDDDK (FLAG)-tag mAb-Magnetic Agarose (M185-10R), DDDDK-tag mAb-horseradish peroxidase-Direct (M185-7; RRID:AB_2687978; 1:2,500 for IB), and human influenza hemagglutinin (HA)-tag mAb-horseradish peroxidase-Direct (M180-7; RRID:AB_11124961; 1:2,500 for IB) were purchased from Medical & Biological Laboratories (Tokyo, Japan). The antibody against Vti1b (611404; RRID:AB_398926; 1:1,000 for IF) was purchased from BD Transduction Laboratories (Franklin Lakes, NJ); anti-mouse IgG (H+L)-CF 488A secondary antibody [20010; 1:2,000 for IF] was purchased from Biotium (Fremont, CA), and anti-Rabbit IgG (H+L)-Alexa Fluor 594 secondary antibody (111-586-144; RRID:AB_2338070; 1:2,000 for IF) was purchased from Jackson ImmunoResearch Laboratories (West Grove, PA).

Cell and tissue culture

HM3KO and MNT-1 human melanoma cells were maintained in DMEM supplemented with 10% fetal bovine serum and antibiotics (Sigma-Aldrich, St. Louis, MO). Normal human epidermal melanocytes (NHEMs) (moderate pigmentation) and a three-dimensional reconstructed human skin model (MEL-300-A) were obtained from Kurabo Industries (Osaka, Japan). NHEMs and the human skin model were maintained in medium 254 containing human melanocyte growth supplement II and long-life maintenance medium (Kurabo Industries), respectively.

Plasmids, small interfering RNA, and their transfection

To generate the Halo-tagged human tyrosinase (*hTYR*) in pFN21A vector (Promega, Madison, WI), HA-tagged *hTYR* in pEF-BOS-3xHA vector (Mizushima and Nagata, 1990), and FLAG-tagged *hTYR* in p3xFLAG-CMV-10 vector (Sigma-Aldrich), cDNA encoding *hTYR* was amplified by PCR using the BCMGS NHT2 plasmid. To generate *hTYR* point mutations at Cysteine⁸, Cysteine³⁵, and Cysteine⁵⁰⁰, altering cysteine to alanine was introduced using a mutagenesis kit (Toyobo, Osaka, Japan) with the following primers: 5'-GCCCTGCTGTGGAGTTCCAGACCTCCG-3' and 5'-GTA CAAACAGCCAGGAGCAT-3' for C8A, 5'-GCCTGTCCA CCGTGGAGCGGGACAGGA-3' and 5'-TTCCTTCTCCAT-CAGTTCCTAGAGGAG-3' for C35A, and 5'-GCCCTG CTGTGGAGTTCCAGACCTCCG-3' and 5'-GTACAAAACAG CCAGGAGCAT-3' for C500A.

For knockdown experiments in HM3KO cells, small interfering RNAs against the following genes and negative (scramble) control were obtained from Cosmo Bio (Tokyo, Japan): 5'-GAACAAUUGUGUUGGAUUUTT for Asp-His-His-Cys (*DHHC*) 2, 5'-GCACAGAUGAGACGGGAAUTT-3' for *DHHC*3, 5'-GAACAAUUGUGUAGGAGAATT-3' for *DHHC*7, GGACCUACUGGAAGUCUAUTT for *DHHC*15, and 5'-ATCCGCGCGATAGTACGTA-3' for negative control.

HM3KO and MNT-1 cells were transfected using Lipofectamine LTX or Lipofectamine 3000 (Thermo Fisher Scientific, Waltham, MA). Briefly, 4×10^5 cells in six-well plates were transfected with 1,000 ng of plasmid. NHEMs were transfected with pCE-puro His₆-Myc-DHHCx plasmids using the electroporator NAPAgene21 (NEPAGENE, Ichikawa, Japan). Briefly, 1×10^6 NHEM/100 μ l culture medium and 10 μ g plasmid were used under the following conditions: voltage, 150 V; pulse width, 50 ms; and two repetitions. A total of 2×10^5 HM3KO cells/60-mm dish were transfected with small interfering RNAs using Oligofectamine (Thermo Fisher Scientific).

Immunoblotting and immunoprecipitation

Cell lysates were separated using SDS-PAGE, followed by immunoblotting. The immunoreactivities of the blots were detected using an ECL-plus (GE Healthcare, Buckinghamshire, United Kingdom) and ChemiDoc XRS with 1-D analysis software (Quantity One, Bio-Rad Laboratories, Hercules, CA) or FUSION SOLO S with Evolution Capt software (Vilber, Paris, France).

For immunoprecipitation (Figure 3g), equal amounts of FLAG-tagged tyrosinase (wild-type or C500A) with HA-tagged ubiquitin were cotransfected into HM3KO cells for 48 hours, after which equal amounts of membrane fraction protein of the cells were incubated with 7.5 μ l of magnetic agarose-conjugated DDDDK (FLAG) antibodies for 2 hours at 4 °C. For immunoprecipitation (Figure 6c), an equal amount of FLAG-tagged tyrosinase (wild-type or C500A) with Myc-tagged DHHC (DHHC2 or DHHC3) or without Myc-tagged DHHC (instead, an equal amount of empty backbone vector) plasmid were cotransfected into COS-7 cells (RRID:CVCL_0224). After 48 hours, cell lysates were incubated with 10 μ l of magnetic agarose-conjugated Myc antibodies for 2 hours at 4 °C. After washing, eluted proteins were analyzed by SDS-PAGE and immunoblotting.

Detection of palmitoylated tyrosinase by acyl-RAC

After the indicated treatment/transfection, cells were collected and washed with Dulbecco's PBS(-). After freeze thawing, the cells were lysed in a lysis buffer (50 mM Tris-hydrogen chloride, 150 mM sodium chloride, 5 mM EDTA, and 1.0% NP-40; pH 7.4) containing a protease inhibitor cocktail (Roche, Basel, Switzerland). After incubating on ice for 10 minutes, the lysates were centrifuged at 20,000g for 15 minutes, and the supernatant was incubated with HE buffer (100 mM 4-(2-hydroxyethyl)-1-piperazineethanesulfonic acid and 5 mM EDTA; pH 7.4) containing 2.5% SDS and 0.1% methyl methanethiosulfonate for blocking free thioester linkages. After incubation at 50 °C for 10 minutes, the proteins were precipitated using three volumes of cold acetone twice. The pellets were resuspended in HES buffer (HE buffer containing 1% SDS), and their protein concentrations were determined

using the BCA protein assay. Equal volumes of proteins (125 µg/150 µl HES buffer) were added to 150 µl of 2 M NH₂OH (hydroxylamine), freshly prepared in 100 mM 4-(2-hydroxyethyl)-1-piperazineethanesulfonic acid and 50 mM EDTA, and adjusted to pH 7.2 using sodium hydroxide or 2 M sodium chloride. Binding reactions were conducted on a rotator at 23 °C for 2 hours. Resins were washed four times with HES buffer. For immunoblotting, elution was performed using 60 µl of an SDS-sample buffer (Bio-Rad Laboratories) with 5% 2-mercaptoethanol; the eluate was heated at 95 °C for 10 minutes, followed by SDS-PAGE and immunoblotting.

Detection of palmitoylated tyrosinase through metabolic labeling and click chemistry

HM3KO cells were cultured in 60-mm dishes and incubated with 50 µM 17-octadecynoic acid (34450-18-5, Cayman Chemical, Ann Arbor, MI) in a growth medium for 4 hours. Cells were then washed three times with ice-cold PBS and solubilized through sonication in HN buffer (50 mM 4-[2-hydroxyethyl]-1-piperazineethanesulfonic acid, 150 mM sodium chloride, pH 7.4) containing protease inhibitor cocktail (03969-21, Nacalai tesque, Kyoto, Japan). To concentrate the membrane fraction, cell lysates were centrifuged at 20,000g for 15 minutes at 4 °C. The pellets were resuspended in HN buffer containing 4% SDS and subjected to methanol–chloroform precipitation to remove the excess probe and other probe-incorporated metabolites. The pellets were then resuspended in 1% SDS in HN buffer. After measuring the protein concentration using the BCA protein assay, lysate containing 150 µg of membrane protein was adjusted to a reaction volume of 150 µl containing 100 µM azide-PEG3-biotin (762024, Merck, Darmstadt, Germany), 1 µM neutralized tris(2-carboxyethyl)phosphine (77720, Thermo Fisher Scientific), 83.5 µM tris(1-benzyl-1H-1,2,3-triazol-4-yl)methylamine dissolved in DMSO/tert-butanol (20:80%, 678937, Merck), and 1 µM CuSO₄ (final reagent volume adjusted with HN buffer) and incubated for 1 hour at room temperature. The proteins were then precipitated with chloroform–methanol, and the resultant pellets were dissolved in 40 µl of 1% SDS in HN buffer. A total of 30 µg of solubilized proteins was retained to assess total input, whereas the remaining 120 µg was incubated with 10 µl of streptavidin-agarose (S1638, Merck) in 400 µl of HN buffer for 2.5 hours at room temperature. After washing, the biotinylated proteins were eluted with an SDS-sample buffer at 95 °C for 5 minutes. For immunoblotting analysis, the eluted proteins were separated using SDS-PAGE and visualized with antityrosinase antibody.

RT-qPCR

Total RNA was isolated using the RNeasy Mini Kit (Qiagen, Hilden, Germany). First-strand cDNA was synthesized from 1.0 µg of total RNA using a ReverTra Ace qPCR RT kit (Toyobo). RT-qPCR was performed using THUNDERBIRD SYBR qPCR Mix (Toyobo) and LightCycler 480 (Roche). Tyrosinase mRNA levels were expressed relative to that of *GAPDH*. The following primers (Sigma-Aldrich) were used:

5'-CACCATGCTCCTGGCTG-3' and 5'-TTATAATGGCTCTGATACAACGTGTGG-3' for tyrosinase, 5'-CCACCCATGGCAAATTC-3' and 5'-TGGGATTTCCATTGATGTGACAAG-3' for *GAPDH*, 5'-AGCCAAGGATCTTCCCATCT-3' and 5'-TCACAGACGGAGCAGTGATG-3' for *DHHC2*, 5'-GGTGTA-CAAGTGCCCCAAAT-3' and 5'-GGACAGTGGTGGTCCATCTT-3' for *DHHC3*, 5'-GGTCAACGGGGTCATCTTTA and 5'-TTTCGTAGCGTTTCTTTGG-3' for *DHHC7*, and 5'-TGCCAGTGCTCGTTATTGTC-3' and 5'-AGAACACAAAGATGGCATGGT-3' for *DHHC15*.

Semiquantitative RT-PCR

Total RNA was isolated from NHEMs and HM3KO cells using RNeasy Mini. Semiquantitative RT-PCR was performed using 0.4 µg of total RNA and the SuperScript III One-Step RT-PCR kit (Thermo Fisher Scientific). The following primers were used: 5'-CATCAGGAAGTTCTTAGGCGAG-3' and 5'-ACATTATCACAGACGGAGCAG-3' for *DHHC2*, 5'-ACAAGTGTGTAGGCGAGAAC-3' and 5'-AGAGAAGGAGCTGCACTTTG-3' for *DHHC3*, 5'-CTTCTGGTACTCTGTGGTCAAC-3' and 5'-CTTTCGTAGCGTTTCTTTGG-3' for *DHHC7*, and 5'-TGCTCGTTATTGCTCCTCGTC-3' and 5'-CTCCAGTAGGTCCAGGTAAAG-3' for *DHHC15*.

Screening for tyrosinase-specific DHHCs

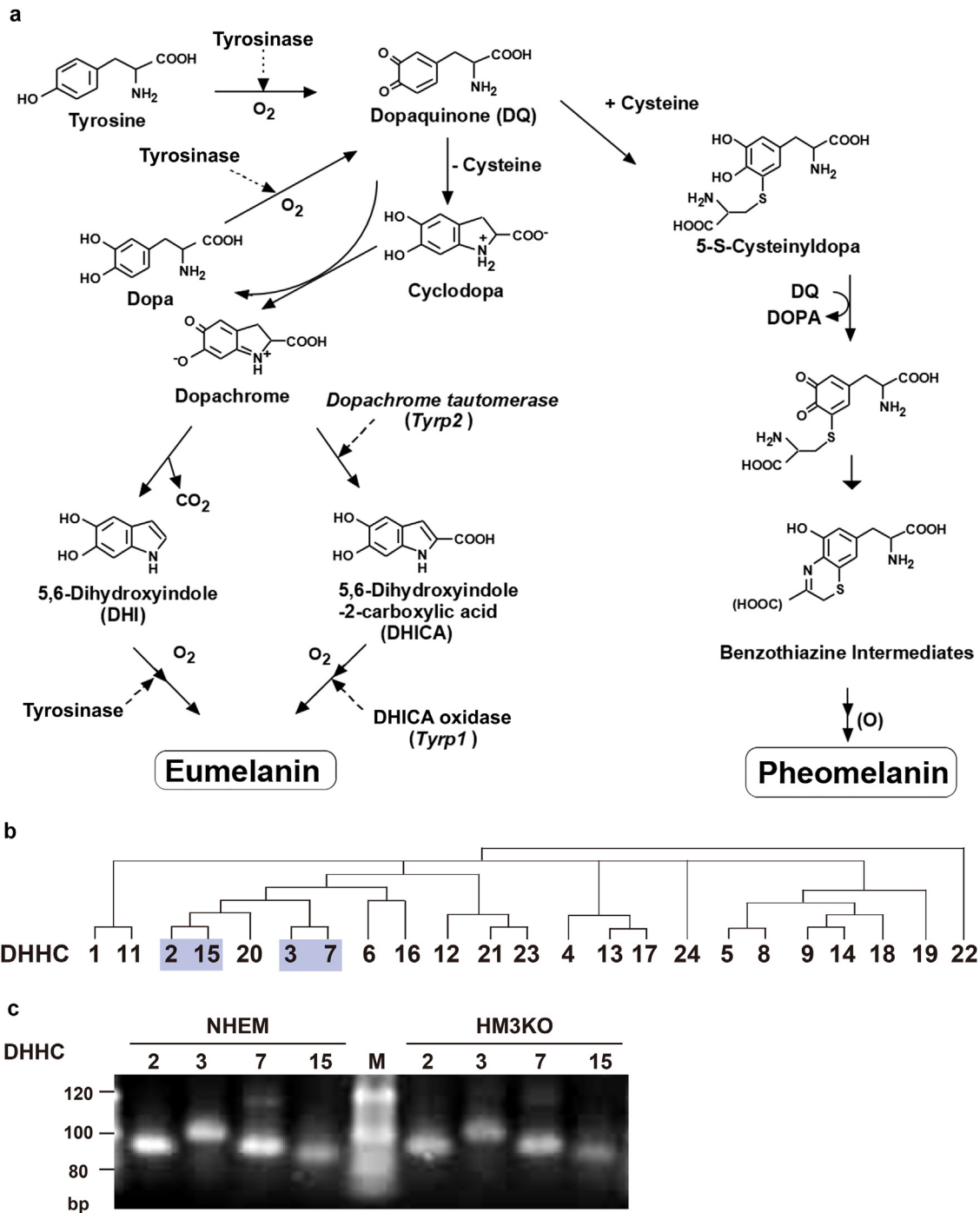
Human embryonic kidney 293T cells (*RRID:CVCL_0063*; 2.5 × 10⁵ cells/12-well plate) were cultured for 16–20 hours in DMEM containing 10% FBS. HA-tagged tyrosinase and DHHC1–23 plasmids (Fukata et al., 2006) were cotransfected. Metabolic labeling was performed using 0.2 mCi/ml (³H)-palmitate (PerkinElmer, Branchburg, NJ) for 4 hours. After incubation, cells were lysed with SDS-sample buffer and separated using SDS-PAGE. After fixing the gels for 30 minutes in a fixing solution (isopropanol: water: acetic acid = 25: 65: 10), they were treated with amplification buffer (1 M sodium salicylate/15% ethanol), dried under vacuum, and exposed to an X-ray film. Radiolabeled bands were scanned in the autoradiograph and analyzed using the National Institutes of Health (Bethesda, MD) software.

Statistical analysis

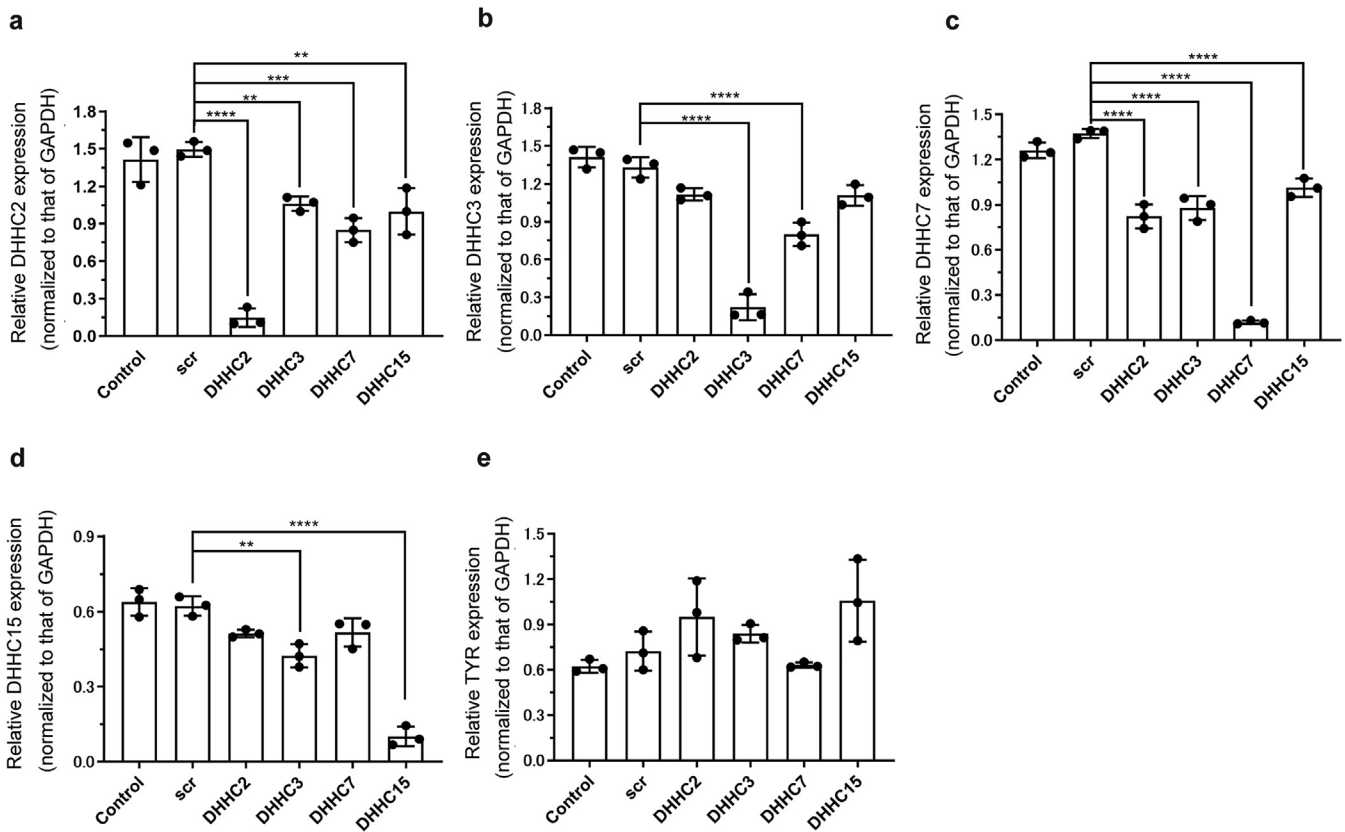
Data are presented as the mean ± SD. For comparisons between two groups, unpaired two-tailed Student's *t*-test was used. For comparisons between more than two groups, one-way or two-way ANOVA was performed, followed by Tukey's or Bonferroni's posthoc tests for pairwise group differences. Statistical analyses were performed using Prism 7.0 software (GraphPad Software, La Jolla, CA). *P* < 0.05 was considered significant.

SUPPLEMENTARY REFERENCES

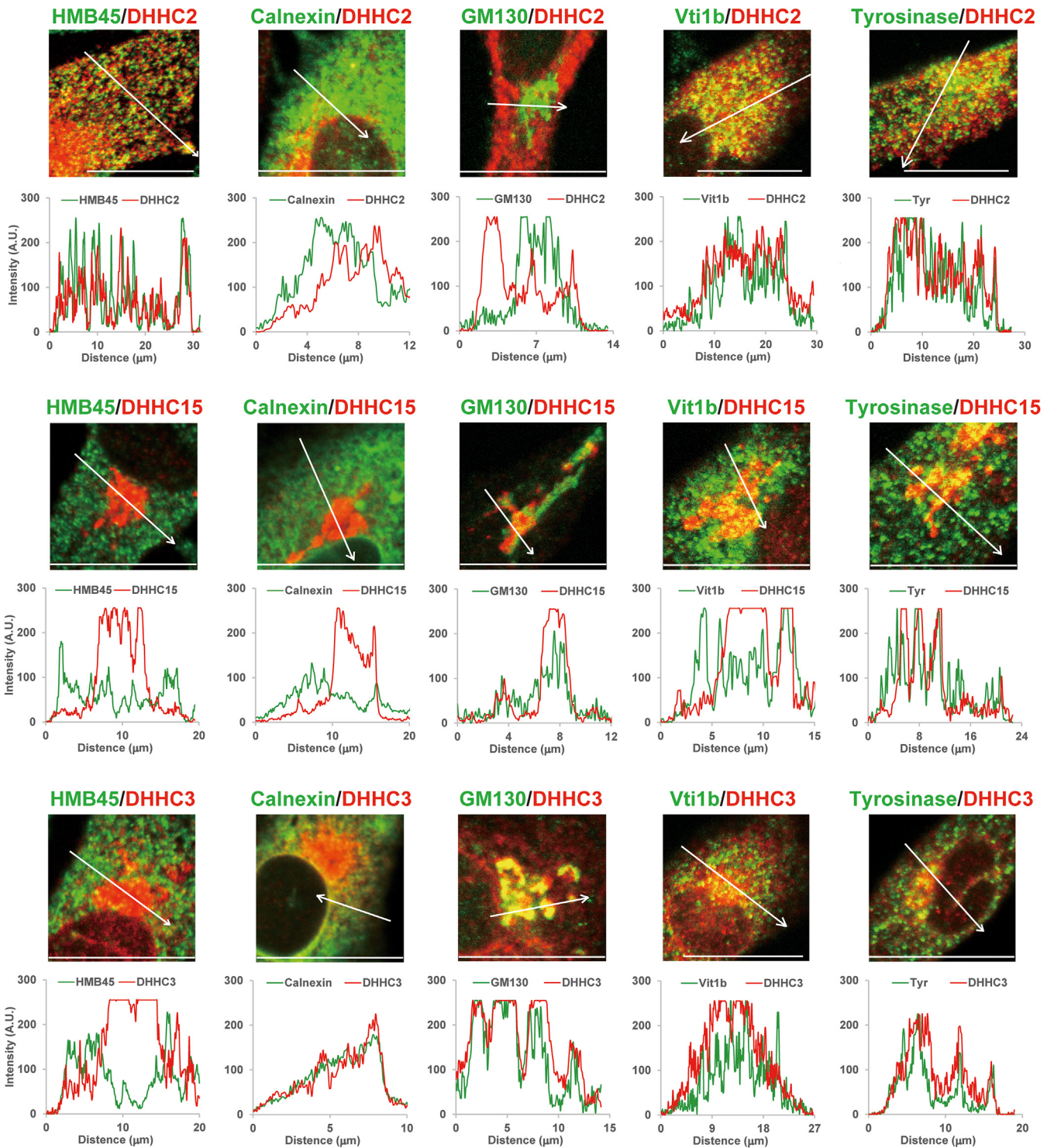
- Fukata Y, Iwanaga T, Fukata M. Systematic screening for palmitoyl transferase activity of the DHHC protein family in mammalian cells. *Methods* 2006;40:177–82.
- Korycka J, Łach A, Heger E, Bogusławska DM, Wolny M, Toporkiewicz M, et al. Human DHHC proteins: a spotlight on the hidden player of palmitoylation. *Eur J Cell Biol* 2012;91:107–17.
- Mizushima S, Nagata S. pEF-BOS, a powerful mammalian expression vector. *Nucleic Acids Res* 1990;18:5322.



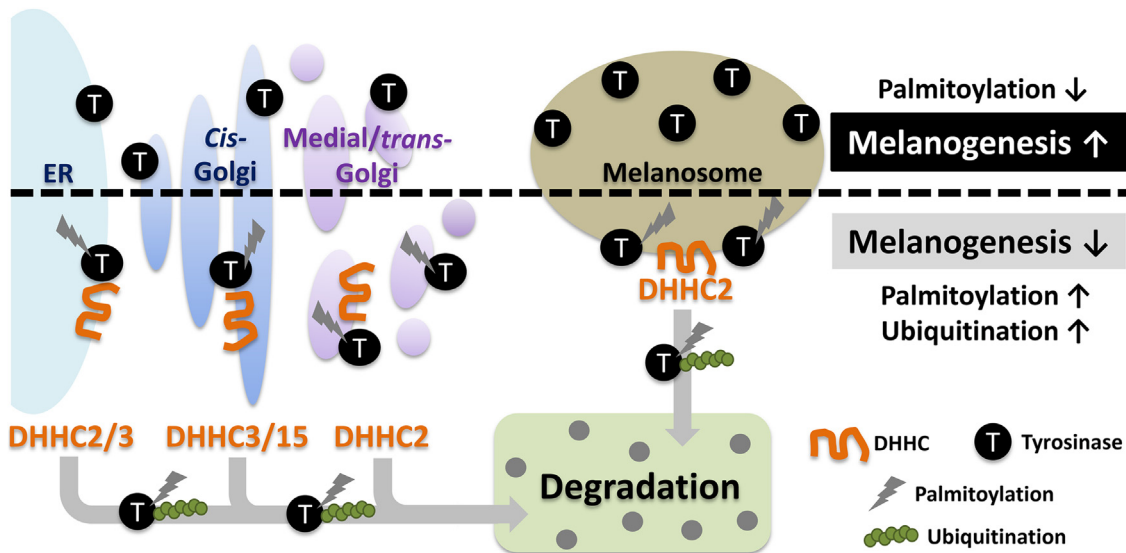
Supplementary Figure S1. Melanin synthesis pathway, the phylogenetic tree of the human DHHC protein family, and mRNA expression of *DHHC2*, *DHHC3*, *DHHC7*, and *DHHC15* in NHEMs and HM3KO cells. (a) Illustration of melanin (eumelanin and pheomelanin) synthesis pathway. (b) Phylogenetic tree of the human DHHC protein family. DHHC2 and 15 and DHHC3 and 7 belong to the same subfamilies (Korycka et al., 2012). (c) Semiquantitative RT-PCR was performed using total RNA from NHEMs and HM3KO cells; *DHHC2*-, *DHHC3*-, *DHHC7*-, and *DHHC15*-specific primers; and a one-step SuperScript RT-PCR kit. *DHHC2*, *DHHC3*, *DHHC7*, and *DHHC15* mRNAs were expressed in both NHEMs and HM3KO cells. M denotes DNA ladder marker. DHHC, Asp-His-His-Cys; NHEM, normal human epidermal melanocyte.



Supplementary Figure S2. Effects of DHHC2, DHHC3, DHHC7, DHHC15 siRNAs on mRNA expression levels of DHHC2, DHHC3, DHHC7, DHHC15, and tyrosinase. HM3KO cells were transfected with either scr or DHHC2, DHHC3, DHHC7, or DHHC15 siRNA. Three days after siRNA transfection, mRNA expression levels of (a) *DHHC2*, **** $P < 0.0001$ (*DHHC2*), ** $P = 0.0089$ (*DHHC3*), *** $P = 0.0003$ (*DHHC7*), and ** $P = 0.0032$ (*DHHC15*); (b) *DHHC3*, **** $P < 0.0001$; (c) *DHHC7*, **** $P < 0.0001$; (d) *DHHC15*, ** $P = 0.0015$ (*DHHC3*) and **** $P < 0.0001$ (*DHHC15*); and (e) tyrosinase (*TYR*) were analyzed using RT-qPCR. The *DHHC* mRNA expression was normalized to that of *GAPDH*. $n = 3$. Analysis was performed with one-way ANOVA with Tukey's posthoc test. DHHC, Asp-His-His-Cys; scr, scramble; siRNA, small interfering RNA.



Supplementary Figure S3. Intracellular localization of DHCs in NHEMs. Magnified images of Figures 5 and 6a are shown. The fluorescence intensity profile across the arrow for both green and red channels was analyzed using Zen software, 2010 (Carl Zeiss, Oberkochen, Germany) and shown in the graph. Bars = 20 µm. DHC, Asp-His-His-Cys; NHEM, normal human epidermal melanocyte.



Supplementary Figure S4. A regulation model of melanin synthesis through palmitoylation-mediated tyrosinase degradation. Tyrosinase is synthesized in the ER, matured in the Golgi apparatus, and trafficked to melanosomes through the endosomes. During this process, tyrosinase may be palmitoylated in the ER by DHHC2 and DHHC3; in the Golgi apparatus by DHHC2, DHHC3, and DHHC15; and in melanosomes by DHHC2. Tyrosinase palmitoylation accelerates its ubiquitination and degradation, thereby downregulating melanogenesis. Conversely, inhibition of tyrosinase palmitoylation increases tyrosinase stability and melanogenesis. DHHC, Asp-His-His-Cys; ER, endoplasmic reticulum.